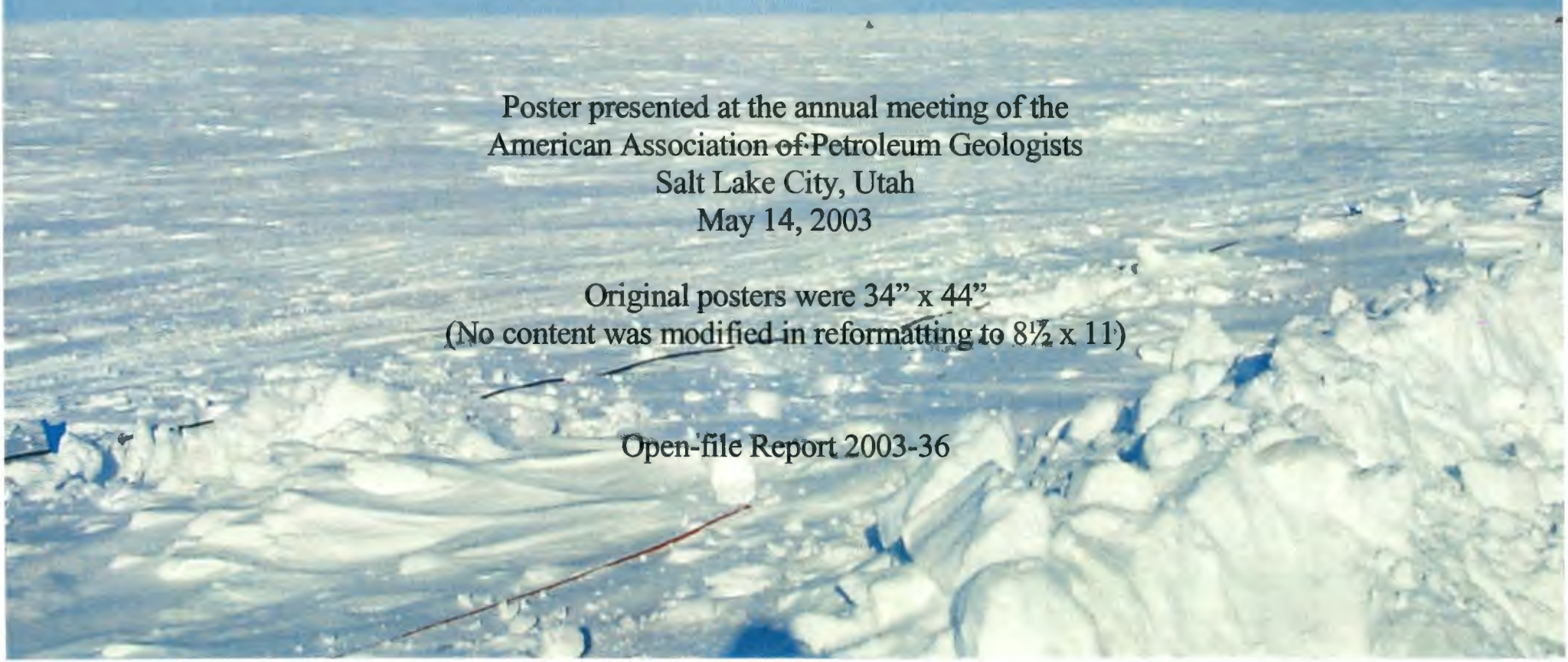
High-Resolution Seismic Imaging of the Hydrate Stability Zone: Mallik, Canada

by
Richard D. Miller, Kansas Geological Survey, Lawrence, Kansas
James A. Hunter, Geological Survey of Canada, Ottawa, Ontario, Canada
William E. Doll, Oak Ridge National Laboratory, Oak Ridge, Tennessee
Bradley J. Carr, Geophex Ltd, Raleigh, North Carolina
Ron L. Good, Geological Survey of Canada, Ottawa, Ontario, Canada
Robert A. Burns, Geological Survey of Canada, Ottawa, Ontario, Canada
David R. Laflen, , Kansas Geological Survey, Lawrence, Kansas
Marten Douma, Geological Survey of Canada, Ottawa, Ontario, Canada
Timothy S. Collett, U.S. Geological Survey, Denver, Colorado



Poster presented at the annual meeting of the
American Association of Petroleum Geologists
Salt Lake City, Utah
May 14, 2003

Original posters were 34" x 44"
(No content was modified in reformatting to 8½ x 11)

Open-file Report 2003-36

High-Resolution Seismic Imaging of the Hydrate Stability Zone: Mallik, Canada

Richard D. Miller,* James A. Hunter,** William E. Doll,† Bradley J. Carr,‡ Ron L. Good,** Robert A. Burns,** David R. Laflen,* Marten Douma,** and Timothy S. Collett‡‡
*Kansas Geological Survey, 1930 Constant Avenue, Lawrence, Kansas 66047-3726
**Geological Survey of Canada, 601 Booth St., Ottawa, Ontario, Canada K1A 0E8
†Oak Ridge National Laboratory, P.O. Box 2008, Oak Ridge, Tennessee 37831-6400
‡Geophex Ltd., 605 Mercury St., Raleigh, North Carolina 27603-2343
‡‡U.S. Geological Survey, Denver Federal Center, MS-939, Denver, Colorado 80225

Introduction

In March, 1999, a combined geophysical field team (Figure 1) from the Kansas Geological Survey, Oak Ridge National Laboratory, and the Geological Survey of Canada, performed some experimental high resolution seismic testing at the Mallik drill site in the Mackenzie Delta, Northwest Territories, where drilling and sampling had previously identified gas hydrates at depth beneath a thick permafrost zone (Figure 2).

In this presentation, we show data from this seismic test, along with comparisons and observations significant to the effective use of high resolution imaging and important considerations about high resolution operations in this environment. Included are discussions and examples based on previous studies at this site, data acquisition, processing, correlation of results with other data sets and some recommendations for future surveying.



Figure 1. Scientists deploying geophones beneath snow cover near Mallik well locations.

Background Information

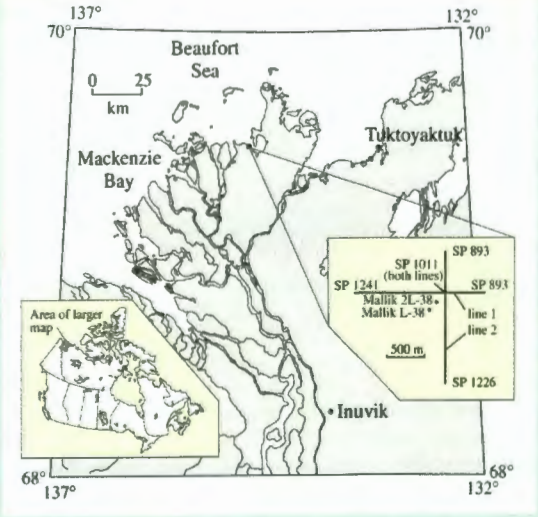


Figure 2. Site map showing relative locations of lines and area relative to Canada.

Large volumes of natural gas can be contained in small volumes of clathrate hydrate, an ice-like substance that is found in the pore spaces of sediments and sedimentary rocks worldwide where specific high pressure and low temperature conditions exist.

The detection and delineation of natural gas hydrates are important since:

– they represent a significant energy supply if they can be economically produced;

– they are recognized as drilling hazard because of high dissociation pressures produced;

– in the long term, their dissociation in the sea bottom and on land may have an adverse impact on global climate should geothermal gradients change in some areas of the world.

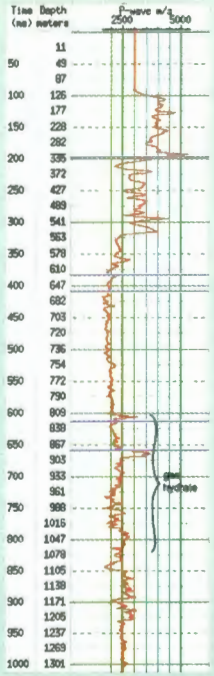


Figure 3. P-wave sonic log in L-38 with time to depth conversion and key intervals interpreted.

Typical conditions for hydrates formation are met in subsea bottom sediments of continental margins between depths of 1200 and 1500 m below sea surface, and, in polar regions on land where permafrost and significantly lower ground temperatures allow their formation from shallow depths of 200 m or less to depths beyond 1000 m. Where significant gas hydrates are found in the pore spaces of sedimentary rocks, measured compressional- (P-)wave velocities of the rock resemble those under ice-bonded permafrost conditions (Figure 3). Where permafrost and gas hydrate pressure-temperature stability zones differ, then seismic velocities can be used confidently for mapping purposes (e.g., below the base of permafrost).

The Field Site

The field site for this test is within the Mallik gas field located at the edge of the Mackenzie River delta approximately 130 km north of the nearest settlement of Inuvik (Figure 2) accessible only by ice road with heavy equipment (Figure 4). The terrain is basically flat, white, and cold in winter and flat, treeless, and marshy in summer.

The Mackenzie delta area contains a thick sequence of oil and gas bearing Tertiary and Cretaceous sedimentary rock capped by Quaternary sediments. Permafrost thickness varies between 0 and 650 meters or more depending on the surface influence of the Mackenzie River and the Arctic Ocean. At the Mallik L-38 site the base of ice bonding is interpreted to be at approximately 600 m depth. The depth to the base of the hydrate stability zone as derived from geothermal temperatures measured in exploration wells (Majorowicz and Smith, 1999) in the area is estimated to be at approximately 1200 m at the Mallik L-38 site.



Figure 4. Ice road accessing field site from Inuvik, Northwest Territory, Canada.

The Mallik area was first drilled by Imperial Oil Ltd in the early 1970's. This site was chosen for research drilling by the JAPEX/JNOC/GSC gas hydrates research team headed by Dallimore, Uchida, and Collett of the GSC, JAPEX and USGS respectively, based on well logs for Mallik L-38 which indicated the possible presence of gas hydrates at depth beneath the permafrost layer. The Mallik 2L-38 well, drilled in January-February of 1998, 102 meters away from the original well, encountered substantial gas hydrates zones within the same depth range with slight variability in apparent thicknesses of the zones within the gas hydrate stability zone. The findings of this most successful drilling program are documented in GSC Bulletin 544 (Dallimore et al., 1999).

Previous Seismic Work

A regional seismic reflection survey obtained by Imperial Oil Ltd in the vicinity of the Mallik site highlighted folded and faulted structures with NW-SE strike (Figure 5). These data were acquired in 1984 and reprocessed as part of the Mallik 2L-38 study published by Collett et al. (1999). This is conventional dynamite seismic data with 40 m group spacing and a nominal fold of 15. The dominant frequencies of reflectors are in the 20-40 Hz range. The zones of gas hydrates and free gas as defined by Collett et al. (1999) are as shown.

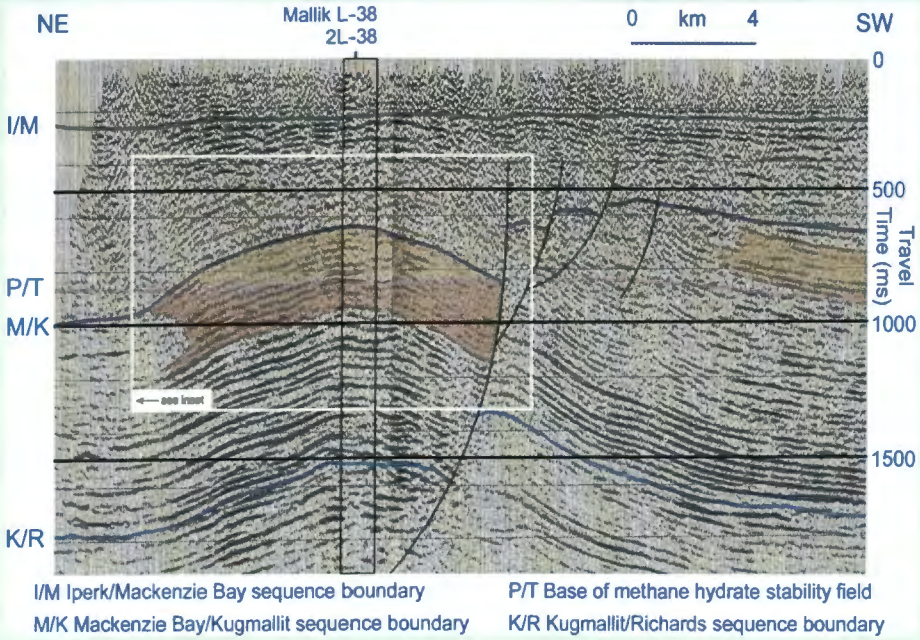


Figure 5. Conventional seismic data reprocessed by Collett et al., 1999.

Geology and Velocity

The Iperk formation: Plio-Pleistocene age—coarse-grained sandy sediments with conglomeratic beds,
The Mackenzie Bay formation: Oligocene-Miocene age—sand dominated with some fine-grained units,
The Kugmallit formation: Oligocene age—interbedded sand and silt units.

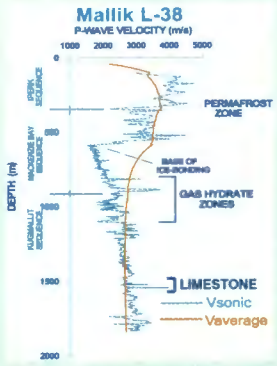


Figure 6. Interval and average velocity logs derived from acoustic and crystal cable logs from the Mallik L-38 well.

All formations are weakly cemented, the Iperk and Mackenzie Bay are ice-bonded or ice bearing within the permafrost zone. Within the permafrost zone, velocities reach as high as 4000+ m/s, generally associated with coarse-grained sediments in grain-to-grain contact with interstitial ice (Figure 6). Note the velocity minimum at approximately 330 m depth associated with the Iperk-Mackenzie Bay boundary. This zone is an essentially a non ice-bonded talik zone which persists throughout the area and is thought to be a result of past permafrost degradation and reformation. The base of permafrost is a velocity gradient responding to the change in interstitial ice in the sediments.

Large velocity contrasts can be seen in the zone of gas hydrates between 810 and 1100 m depth, as these ice-like materials fill the pore space in a manner similar to ice bonding within the permafrost. Similar hydrate conditions exist in both Mallik L-38 and 2L-38 (Figure 7). Dramatic changes in permafrost velocity that result from changes in clay content of unconsolidated sediments can produce static time shifts in reflection that resemble structure (Figure 8). These changes in material velocity can alter the apparent velocity by as much as 25 percent. Therefore, Vaverage as predicted in Figure 6 could only be used as a general range of velocities but detailed station-by-station analysis was necessary to accurately correct the seismic data.

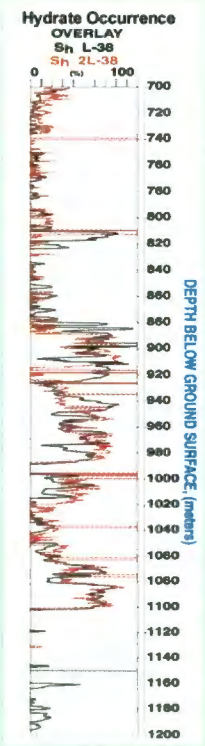


Figure 7. (right) Overlay of percentage of hydrate occurrence in Mallik L-38 and 2L-38 (from Tim Collett, USGS).

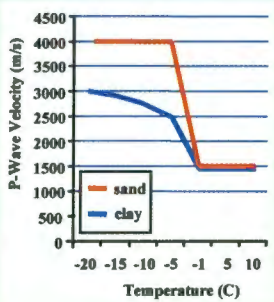


Figure 8. Change in velocity relative to permafrost termerature and percent clay content.

Reflections should be generated from large velocity contrasts between 200 and 400 ms within the permafrost section. High velocities zones associated with the gas hydrate layers between 850 to 1050 m depth should generate strong reflections in the 600 to 800 ms range. Lateral changes in reflection amplitude could relate to hydrate concentration or changes in clay content.

Reflections within the permafrost are clearly visible on the conventional seismic section as well as several events in the 650-1050 ms range likely associated with the gas hydrate layers (Figure 5). The frequency content is such that individual layering cannot be delineated. From this section, it is apparent that reflections associated with hydrate zones are not continuous but are concentrated at the top of the anticlinal form.

1999 High Resolution Seismic Survey

The 1999 testing is concentrated in small area approximately 1 km wide at the apex of the anticline centered on the Mallik 2L-38 well where we have attempted to image the upper 1500 m of the section (approximate 1 second two-way travel time) (Figure 5).

Two orthogonal seismic lines (N-S and E-W, Figure 3) were surveyed in, so that the original 1972 well Mallik L-38 and the hydrate well Mallik 2L-38 were midway between the two lines. The positions of the lines were chosen after careful examination of the air photos of the area, in an attempt to keep the line positioned on firm ground and avoiding small ponds or river channels as much as possible. This was done to minimize potential static anomalies due to variable, near-surface permafrost conditions (hence velocity anomalies) (Figure 9). Permafrost temperatures, ice contents and P-wave velocities can vary due to presence of ponding. In the summertime, this area is swampy and thermal anomalies (hence velocity anomalies) within the permafrost abound. Such anomalies are minimized by late winter (March-April). Data acquisition procedures that have been developed for near-surface applications were incorporated in this survey, and were essential to the success of this project.

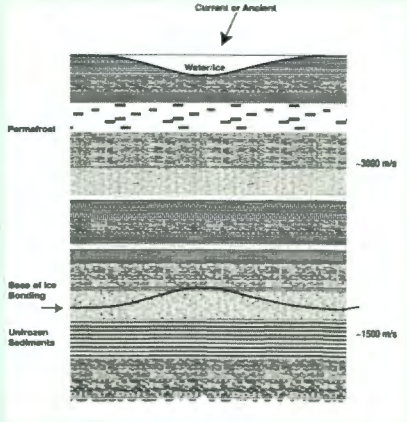


Figure 9. Thermal anomaly at the base of permafrost beneath water can cause large changes in velocity and result in apparent structures on stacked seismic sections.

Leveling to ground and clearing off sod was not allowed by the land use permits since permafrost degradation would result. The lines were cleared, leaving as much as 20 to 30 cm of packed snow protecting the ground surface (Figure 10).

Seismic Sources

Small dynamite sources at shallow depths on such a small spacing would be logistically difficult and probably forbidden in such an environmentally sensitive area. However, we did test the 8-gauge in-hole Buffalo gun using a 500 grain black powder blank shell, (the largest shell manufactured by Betsy Seisgun), in a shallow 2-inch bored hole. In frozen ground, with the gun tamped by snow, energy transmission into the formation was found to be poor. Although somewhat useable records were obtained with this device, most of the energy was going into the air. If it were logistically and fiscally possible, it is very likely that freezing the gun in place would have provided significant energy and frequency enhancement.



Figure 10 is an aerial picture of Line 1 looking easterward to the camp near the apex of the lines.

The source selected for this work was a winterized IVI Minivib, supplied by Eagle Geophysics of Calgary as shown in Figure 11. Each day the line had to be cleared of snow that blew in to the source path (Figure 12). This source can be operated in both vertical (P-wave) mode as well as in horizontal (SH-wave) mode. The area beneath the vibrator pad was hand-cleared of all snow, allowing direct coupling of the pad to ice or frozen sediments as shown in Figure 13. A significant drop on total energy and frequency content was observed at vibration points where the pad was coupled to the ground through snow.



Figure 11. IVI Minivib with recording shack in background and cables in foreground. Inset is a close-up of the 150 kg mass and baseplate.

A total of six sweeps were recorded for close offset data (50-500 m offsets), and eight sweeps were recorded for long offset data (approximately 500-1000 m offsets). Each sweep was recorded individually and uncorrelated, thus providing maximum flexibility for experimentation during processing with vertical stacking and precorrelation processing. A 10-second 20-200 Hz up-sweep was generated for the P-wave data.



Figure 12. Loader with V-blade to clear path for vib. No ground contact could be made, so a thin 15-30 cm layer of snow isolated the source from the frozen ground.



Figure 13a. (above right) Hand dug to frozen ground to enhance coupling of vibrator pad.

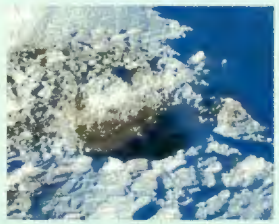


Figure 13b. (right) Hole dug to frozen ground, sized to allow 1-m diameter circular pad to couple flat to ground.



Figure 14. Deployment of parallel strings of five Mark Products L28A 30 Hz geophones in one hole against three L28E 40 Hz geophones in the other hole. Electric drills powered by gasoline generators were used to drill pilot holes for inserting geophones with conventional spikes into the frozen ground. The ground was melted during drilling and therefore once the spike was inserted it quickly froze in place.

Geophone Selection and Placement

Different geophones were tested (Figure 14). Analysis of these data suggested that the 30 Hz vertical geophones were optimum for this site and that these higher-frequency geophones (higher than most conventional 8 to 15 Hz geophones) were essential to the recording of the higher frequency signal necessary to discern layers as thin as 10 m.

Array and Spread Geometry

To ensure good coupling, holes for the geophone spikes were drilled with a power drill (Figure 15), and the geophones were effectively frozen into the ground. Experience has indicated that standard ice base plates do not provide sufficient coupling for low energy high frequency reflection surveying in these conditions. The five geophones per trace were placed side by side in one hole dug through the snow to ground level (Figure 16). Blowing snow conditions prevailed most of the time and the holes quickly filled in providing excellent reduction of wind noise (Figure 17).



Figure 15. Geophones frozen into place using electric drill and masonry bit.



Figure 16. Individual geophone pits hand dug through packed snow to avoid disturbing ground and vegetation.



Figure 17. Geophones were frozen to ground and snow muffled wind and source noise.

The geophone spread geometry consists of nominal 96 channel off<end shooting with 5 meter group spacing. Two source-first trace offsets were used, 50 and 520 m (Figure 18), resulting in shot gathers with the source-to-furthest offset of almost 1 km (Figure 19). Source stations were separated by 10 m and the source was offset from the receivers by 10 m (Figure 20).

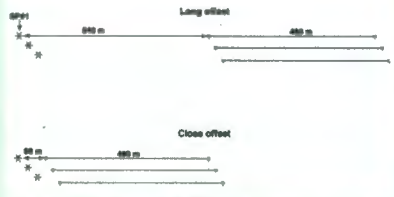


Figure 18. Acquisition geometry that minimized number of recording channels, optimized spread length, and maximized offset.

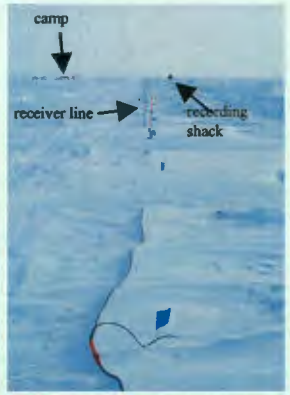


Figure 19. Recording shack, receiver line, and camp.



Figure 20. Source line 10 m from receiver line, source relative to receivers.

Recording Parameters

Data from 94 receivers were recorded for each shot. Data channels to be recorded by the seismograph were selected using a 240-channel roll-along switch (Figure 21). The vibrator was controlled by Pelton Advance II electronics outputting both ground force and the reference. Two Geometrics R-48 StrataViews were networked together with a standard record length of 12.3 seconds and a sample rate of 1 millisecond (Figure 22). Both the source synthetic and ground force were recorded as separate channels, yielding 94 data channels per record stored as SEG-2 format.



Figure 21. Input/Output 240-channel roll-along switch (upper) and Pelton Advance II vibrator controller (lower) mounted in the recording shack.



Figure 22. Networked 48-channel Geometrics Strataview seismographs mounted in the recording shack.



Figure 23. Recording shack was moved along line using the same loader used to clear the source line.



Figure 24. Recording shack deployed offline several 10s of meters to minimize noise. Generator used for heat was located 50 m offline and was cycled off and on to keep noise at a minimum.

With the small footprint, portable nature of this seismic project, assembling equipment and appropriate operational accommodations for that equipment and operators was done with materials available at Inuvik. The portable recording shack was a converted ice box (Figure 23). It was outfitted with shelving and a heater with access ports for seismic cabling. Once deployed it was self-sufficient and could run without generator support for hours at a time (Figure 24).

Inspection of Shot Gathers

Spectral-balanced P-wave shot gathers from the combined offsets possess reflections throughout the upper 1 km at this site (Figure 25). Spectral balancing is basically band limited spiking decon (Figure 26). Note the high-velocity ground roll, around 1500 m/s, generated by surface permafrost conditions. Note also the presence of wide angle reflections out in front of the ground roll, as well as some large events riding on top of the ground roll at near normal incidence. With F-k filtering (Figure 27), some events are enhanced sufficiently to allow confident identification back to near normal incidence. However, large amplitude variations in reflecting events within one shot gather suggest the reflector does not possess physical properties that continue across the length of the spread (about 1 km). This phenomenon is pervasive on all shot gathers.

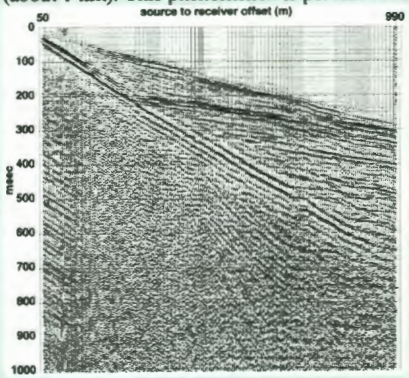


Figure 25. Spectral balanced P-wave shot gather.

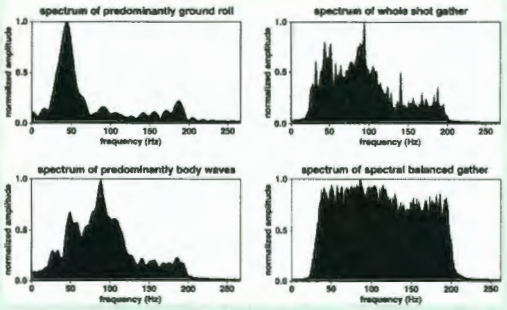


Figure 26. Some of the spectral characteristics of the P-wave data and the spectral balancing performed. Ground roll has predominant energy in the 20-60 Hz range, whereas the body wave energy is in the 40-120 Hz range. The data has been spectrally balanced in the 25-200 Hz range.

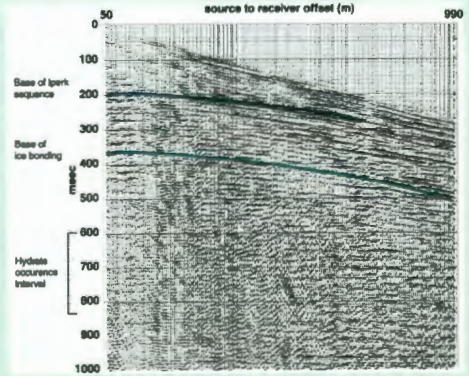


Figure 27. Effectiveness of F-k filter in removing groundroll obvious in Figure 25.

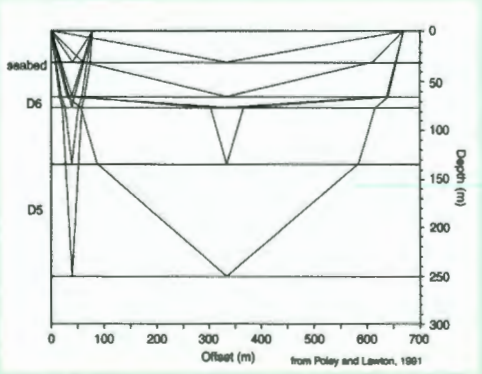


Figure 28. Seismic raypaths in the presence of a high velocity layer like permafrost.

In general the signal-to-noise ratio to 1 second of depth was sufficient to interpret coherent reflection events throughout the depth window of interest from a single shot gather.

There is a question as to which offset window (group of traces) to use in stacking. Commonly we would use all the traces; however, due to the high velocity layer effects which distort the reflection raypath, only the optimum nearest-offset traces were used (Figure 28), so some of the wider angle reflections are quite prominent.

CMP Processing

The processing steps and flow sequence for the seismic lines are shown in Table 1. Only the inner traces between 25 m and 70 m offset were included in the processing sequence since the near trace reflectors are least affected by refractive effects of high velocity near-surface permafrost zone.

Table 1
CMP Seismic Processing Flow

—SEG-2 to SEG-Y
—roundup into 96 channels
—define geometry
—correlate with synthetic pilot
—bad trace edit
—vertically stack each shot station
—first arrival mute
—air wave/groundroll mute
—match trace polarity
—spectral analysis
—spectral balance
—amplitude balance
—F-k filter (remove events w/ groundroll slope)
—CMP sort
—velocity analysis
—surface consistent statics
—common offset statics
—velocity analysis
—normal moveout correction
—residual statics
—CMP stack
—time variable frequency filter
—AGC scale
—migration filter
—display

Line 2 (N-S)

Normal moveout correlations will be inconsistent with the standard second-order moveout equation. Velocity drops from 4,000 m/s to 1,500 m/s at the base of permafrost. Raypaths for reflection immediately below the permafrost are all near vertical. The example shown here is extreme, but repre-sentative (Figure 28).

CMP processed Line 2 (Figure 29) is easily interpreted with formations and coherent reflections (Figure 30). There is a well-defined large amplitude reflection package associated with the permafrost velocity anomaly at approximately 200 ms two-way travel time. This section appears to have no continuously correlatable reflection events across the section at depths that might be interpreted as one continuous gas hydrate zone. Instead, there appears to be a series of acoustic contrasts, some of which laterally correlate for a few hundred meters.

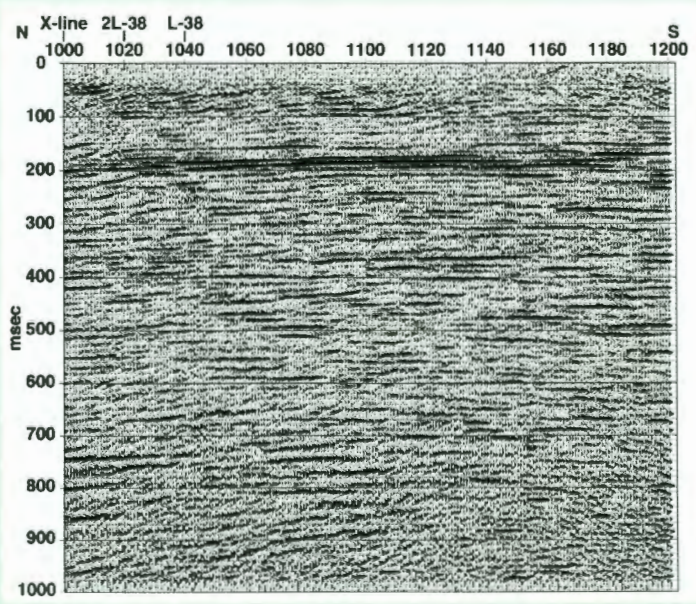


Figure 29. CMP stacked section of north-south line. Data process to maximize coherency. Dominant frequency is around 80 Hz at 1 km depth on CMP stack. At depths less then 30 m dominant frequency is over 150 Hz.

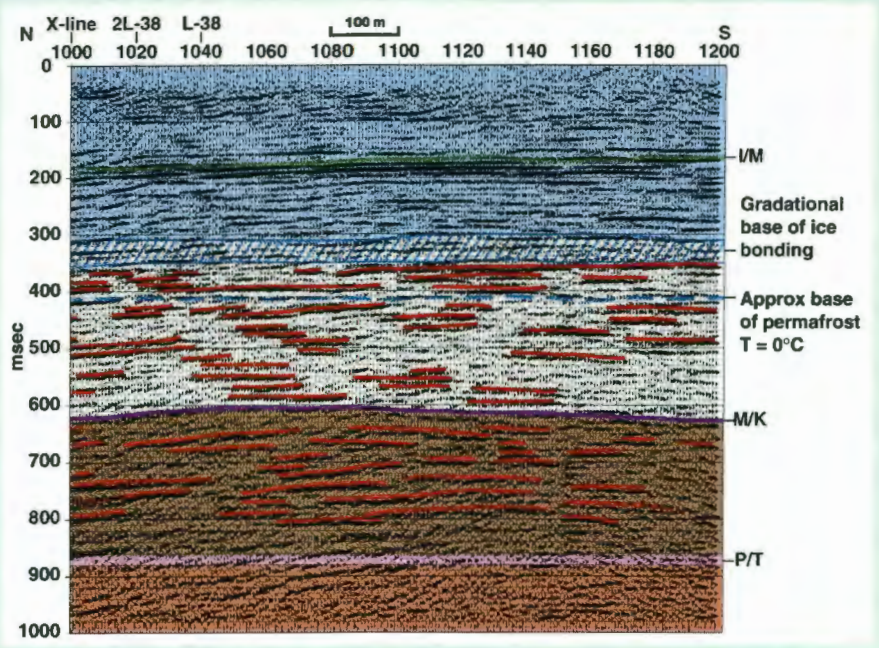


Figure 30. Interpretation of CMP stacked section in Figure 29. Interpretation is based on lateral variations in amplitude with formation interpretations correlated to borehole data.

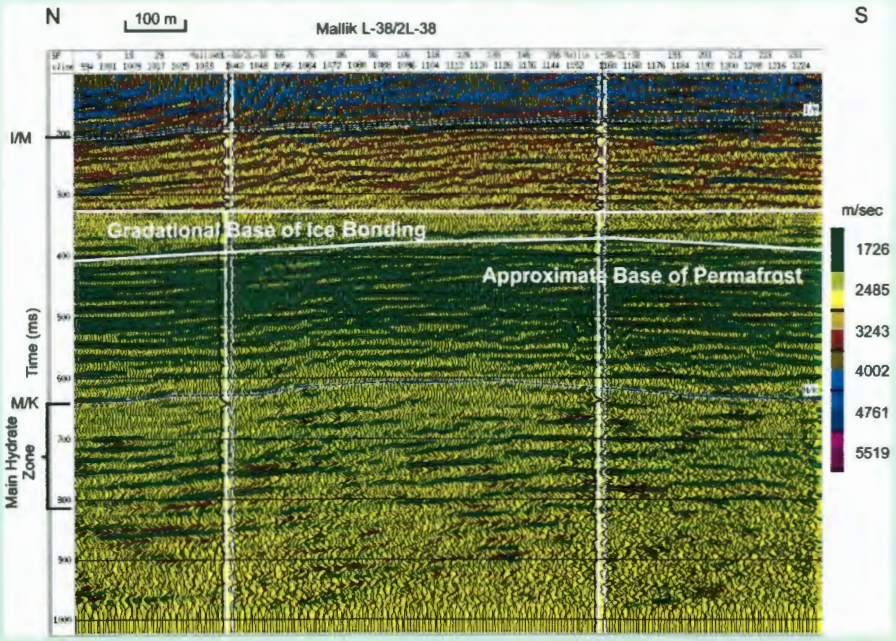


Figure 31. Hampson-Russell velocity-time inversion incorporating the processed seismic data borehole logs from L-38 and a synthetic generated from the borehole sonic. The discontinuous nature of the reflections within the main hydrate zone are extremely evident on this very high-resolution localized scale.

Interpretation

The interpretation of the CMP stacked section is based on a combination of borehole logs and seismic characteristics (Figure 30). The blue zone correlates with permafrost. No clearly distinguishable reflection that can be associated with the base of permafrost. This due to the gradational nature of the base of ice bonding. Within the permafrost is the highest amplitude and most coherent reflection interpreted on these data. This seismic marker bed is the contact between the Iperk and Mackenzie Bay formations. This particular CMP stacked version of the seismic data concentrated on lateral coherency of seismic events and not true amplitude. Therefore interpretations in Figure 30 are also based on coherency. Within the hydrate stability zone several high amplitude, coherent events are highlighted. Most notable is the lack of lateral coherency for distance in excess of a few hundred meters. This could be indicative of hydrate concentrations or changes in the stratigraphy. The very discontinuous nature of the highlighted reflecting events is not intended to suggest major changes in rock types, but more lateral changes in some of the rock properties or port material. With this processing sequence the most dramatic velocity contrasts will dominate the processed sections.

Lateral discontinuity is aptly indicated in Figure 31—a correlation between a composite velocity-depth function for L-38, a synthetic, and the processed data from high resolution Line 2. In general, there is reasonable correlation between synthetics and the observed section throughout the time range. Within the permafrost zone, reflection events are relatively continuous. However, below the base of permafrost and within the hydrate stability zone, the significant events on the section do correlate reasonably well with the synthetics where the well intersects the seismic section, but are not necessarily laterally continuous over long horizontal distances.

Emphasizing this lateral variability in velocity is the Hampson-Russell velocity-time inversion processing (Figure 31). Along this 1 km profile the permafrost possesses reasonably consistent and coherent layering as indicated by the uniformity in the velocity. However, within the hydrate stability zone lateral velocity changes are evident. Noteworthy is the relatively consistent lower velocity zone around 750 msec. This is consistent with 10 m of 0 % hydrate occurrence at 980 m as defined on Figure 7. This zone appears to be reasonably consistent across the entire 1 km. Several "lenses" track across distances of 200 to 300 m before they seem to truncate and then reappear 10 to 100 m away within the main hydrate zone. Subtle changes amplitude evident on the high-resolution CMP sections (Figures 29 and 30) are also evident on the inversion processing (Figure 31).

In Figure 32, showing a travel-time blow-up of the high resolution section, we correlate the hydrate occurrences as given from the well logs (provided by Collett, 2003) with a series of discrete reflection lenses within the known hydrate zone. Here the Fresnel Zone radius is 113 m and the vertical resolution is approximately 10-15 meters.

It should also be reiterated that the wells are 102 m apart, 45 degrees to the line and are between 72 and 144 m off-line from the two high resolution lines; hence correlations should be considered tenuous due to the indicated discontinuous nature of the seismic stratigraphy. However, the general variability evident in drill data is remarkably similar to that observed in the high-resolution data. This apparent correlation in character, cyclicity, and thickness between reflections on the high resolution stacked sections and hydrate layers interpreted in Mallik L-38 and 2L-38 is completely transparent at this scale on the lower resolution, conventionally reprocessed seismic data displayed in Collett et al. (1999). Mapping hydrate layers at higher resolution should be extremely useful and likely essential to any future drilling research, especially those involving deviated holes.

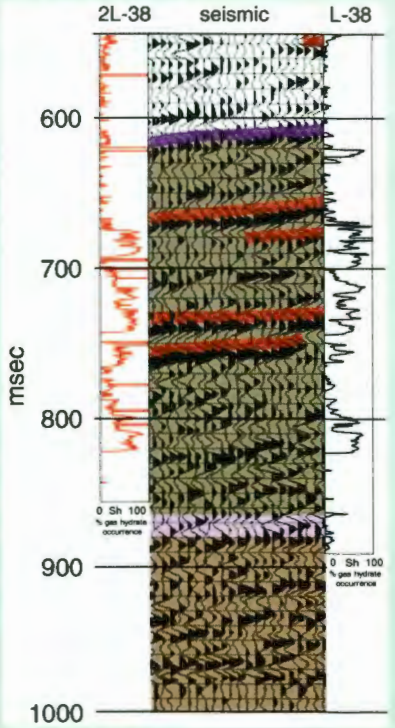


Figure 32. (right) Comparing the high percentage hydrate zones with the seismic data at and between 2L-38 and L-38 provides an extremely revealing correlation between high amplitude events and boundaries between high and low concentrations of hydrates.

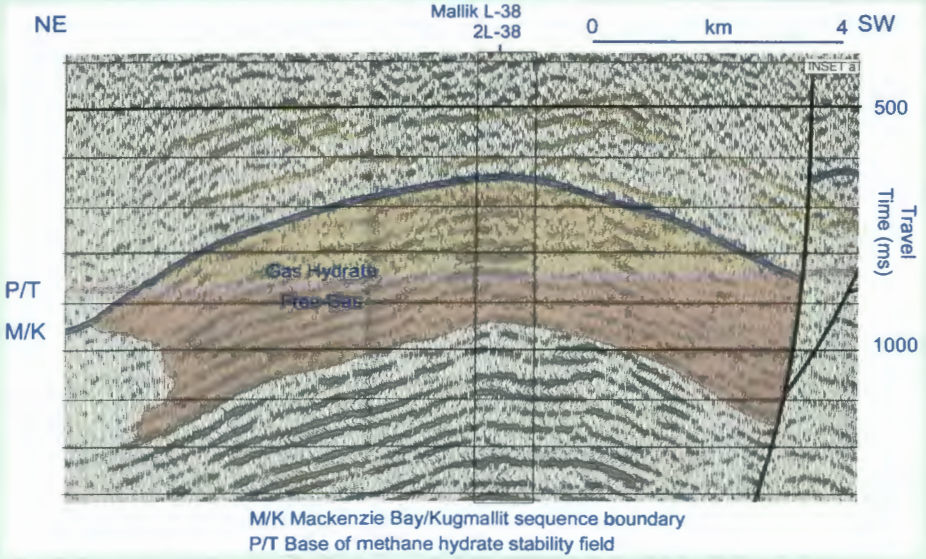


Figure 33. Enlarged section of conventional processed section (Figure 5). Target reflection of high-resolution data is between 600 and 900 ms.

Resolution

As an example of the difference in vertical and horizontal resolution between conventional and our high resolution sections, Figure 33 is a travel-time blow-up of a portion of the regional N-S conventional Esso Line 85251 published by Collett et al. (1999). The events identified as those associated with the hydrate zones in the Mallik wells constitute a few low frequency legs in the apex of the anticlinal seismic stratigraphy; the lowest of these events may also represent the phase boundary between hydrate and free gas, according to Collett et al. (1999). With the observed frequency content (dominant 30 Hz), the second two-way travel time is approximately 196 m. The vertical resolution is approximately 35-40 meters. Note

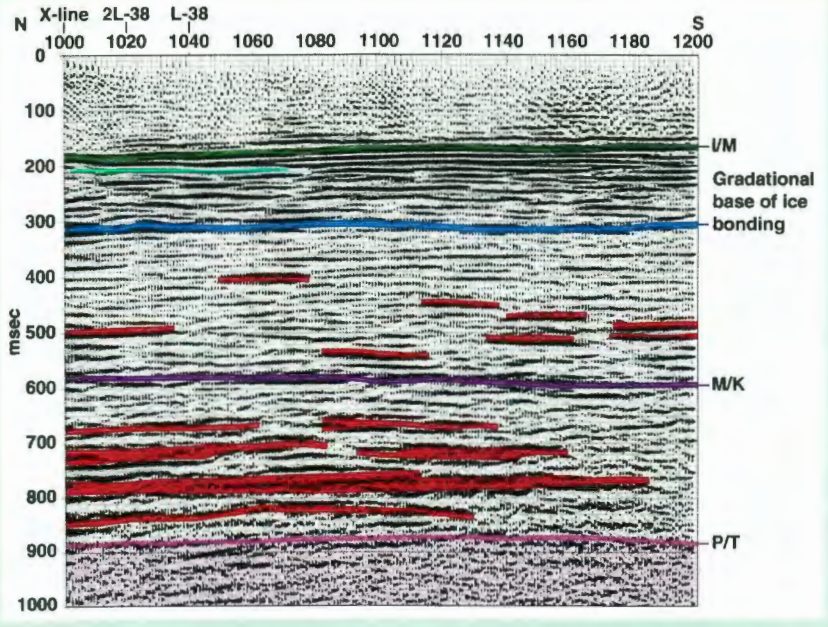


Figure 34. Interpreted CMP section processed true amplitude. Layers within the drill-confirmed gas hydrate zone can be interpreted to be continuous as a packet, but they appear very discontinuous as individual layers.

the shaded vertical strip on the section indicating the I km wide band which is effectively the width of the 1999 high resolution Line 2.

Amplitude processing of the high resolution data provides a consistent but slightly more coherent picture of the hydrate zone (Figure 34). The red highlighted areas are based on higher amplitude only and not necessarily indicative of gas hydrate. Clearly, using this processing scheme there appears to be more connectivity between potential gas hydrate reflections than observed on Figure 30. However, as with the CMP section in Figure 30, the apparent reflecctors with the drill-confirmed hydrate zone change in physical characteristics forming discontinuous lens geometries. Gas hydrate layers defined by Sh borehole logs match very well with this version of the CMP stacked section (Figure 35). Changes in gas hydrate concentrations are likely consistent with geology and therefoe provide a very good correlation to seismic data.

In general, we believe that both the conventional and the high resolution data sets are giving similar results but at markedly different scales of resolution (Figure 36). From a regional perspective, the conventional data of Figure 22 indicates three or four high amplitude events over a vertical time interval of 250 ms which may be associated with hydrate occurrences and which appear to be laterally discontinuous on the scale of 1 km or so. On a more site-specific scale, the high resolution data, with a factor of 2 increase in vertical resolution due to increased frequency content and improved Fresnel zone radii, has mapped laterally discontinuous lenses on the scale of 100 or 200 m or so. Such laterally discontinuous lenses would not be separable as discrete events on the conventional sections, with lower frequencies and larger Fresnel radii.

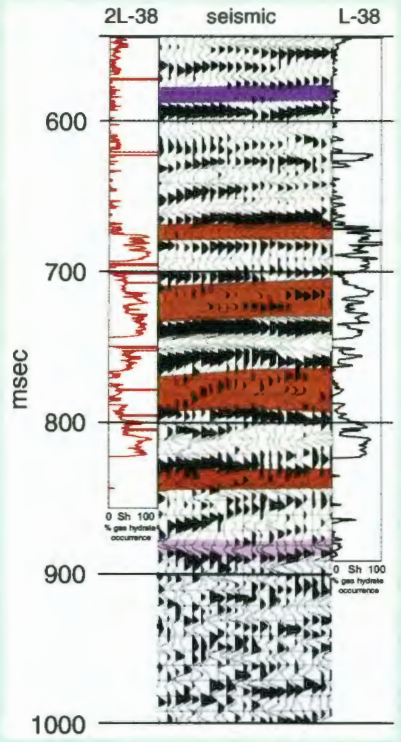


Figure 35. (left) Similar comparison of % gas hydrate occurrence and the high resolution seismic data. Well data properly placed according to seismic station.

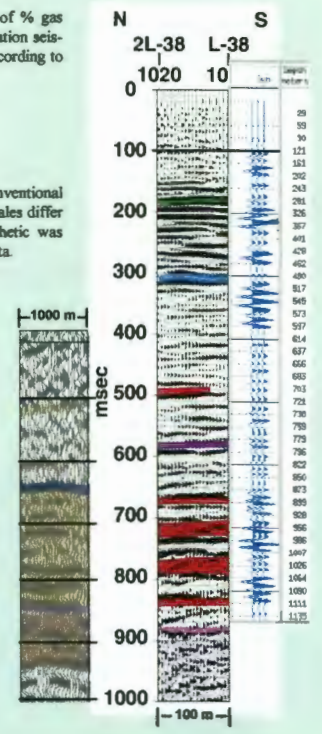


Figure 36. (right) Comparison of conventional and high resolution data. Horizontal scales differ by an order of magnitude. The synthetic was generated from L-38 borehole sonic data.

Conclusions

Hydrates appear to form in regionally correlatable zones within the hydrate stability field but locally vary significantly in thickness and duration across distances of less that 500 m. It is likely local variability is related to changes in physical properties of the reservoir rocks. High resolution seismic reflections appears sensitive to changes in hydrate concentrations in rocks and can be used to map contacts between high and low hydrate concentrations. Conventional seismic data provides a gross overview which can indicate hydrates are present but will not provide the resolution necessary to locate a borehole with high confidence that it will be optimally placed to penetrate a thick sequence of hydrate lenses. This is especially true in the case of production schemes that might involve horizontal drilling.